Improved Frequency Division Multiplexing Process for Motor Drives Data Acquisition using Higher Resolver Excitation Frequency

Igor Ono * **Thyago Estrabis** ** **Gabriel Gentil** ***
Raymundo Cordero **** **Julio C. O. de S. Lescano** †

* *Federal University of Mato Grosso do Sul, MS,
(e-mail:iesdrasono@gmail.com)*
** *Federal University of Rio de Janeiro, RJ
(e-mail:thyago.estrabis@gmail.com)*
*** *Federal University of Rio de Janeiro, RJ
(e-mail:gabrielgent@gmail.com)*
**** *Federal University of Mato Grosso do Sul, MS,
(e-mail:raymundo.garcia@ufms.br)*
† *Federal University of Mato Grosso do Sul, MS,
(e-mail: julio.lescano@hotmail.com).*

Abstract:
Accurate and robust acquisition of angular position and stator currents is critical for developing high-performance three-phase motor drives. Resolver sensor is widely used to measure the motor shaft angular position in harsh conditions. On the other hand, frequency division multiplexing (FDM) is a powerful alternative to send the motor stator current signals and the resolver outputs to the data acquisition system (DAQ) used in three-phase motor drives. In most approaches, the frequency of the resolver excitation voltage is less than the switching frequency of the PWM technique used to control the motor. Hence, the distance between the spectra of the resolver signals and the current signals, which depends on the resolver excitation frequency, is small, increasing the interference of the current signals in the angle estimation (crosstalk). This paper proposes an improved multiplexing approach to reduce the effect of crosstalk in angle estimation. The resolver excitation frequency is 1.5 times the inverter switching frequency so that the resolver outputs are zero when the PWM carrier reaches its valley. Thus, synchronous current sampling can be applied to get the stator current signals, and the effect of crosstalk is reduced in the angle estimation. Simulation results prove that the proposed approach reduces the crosstalk effect in the angle estimation and allows recovering the current signals.

Keywords: Angle tracking observer, data acquisition system, frequency-division multiplexing, resolver, three-phase motor.

1. INTRODUCTION

Robust and accurate measurement of stator currents and angular position/speed is critical to guarantee a good performance of three-phase motor drives based on vector control techniques (Lara et al., 2016; Raja et al., 2017; Ali et al., 2020; Lee et al., 2022). Errors in measurement of the angular position or the stator currents will produce torque ripple that increases the acoustic noise and the mechanical vibrations, and also reduces the motor lifespan.

Resolver sensor is widely used as an angular position sensor in harsh environments. It has good accuracy and more robustness against high temperature and vibrations than other sensors such as encoders (Wang et al., 2019; Saneie et al., 2020; Naderi et al., 2022; Jang et al., 2022). For those reasons, many electric vehicles use resolver. Besides,

a high-performance motor drives data acquisition system (DAQ) should have good accuracy, robustness, and low cost.

Many DAQs apply multiplexing techniques to reduce the complexity and cost of the analog-to-digital (AD) conversion system. Multiplexing is a technique that allows signals from different sources to travel through the same channel (Haykin and Van Veen, 1998). Most DAQs apply time division multiplexing (TDM), where signals from different sources are sent to the input channels of an analog switch. A synchronization system controls this switch to send those signals to a single AD converter at different instants. TDM can be applied to different types of signals. However, the conversion rate of each input signal in TDM is inversely proportional to the number of the multiplexing channels (García et al., 2017).

Frequency division multiplexing (FDM) is another method where band-limited signals with non-overlapping spectra

are multiplexed through an additive process, so those signals occupy different frequency bands (Haykin and Van Veen, 1998). This process creates a new signal which is sent through the communication channel. Usually, FDM requires modulators to shift the spectrum of each signal to different frequency bands. However, the resolver outputs and the current signals have non-overlapping spectra when the resolver excitation frequency and the switching frequency of the inverter that controls the three-phase motor are properly selected. Thus, those signals can be multiplexed in the frequency domain through an analog adder (García et al., 2017; Modesto et al., 2020; García et al., 2021). FDM has many advantages over TDM in data acquisition:

- FDM does not require synchronization.
- FDM allows for using a faster AD conversion rate as the signals are simultaneously sent to the AD conversion system.
- When modulators are not required (as in this case), the multiplexing circuit used in FDM (adders) is simpler than the hardware used in TDM (analog switch and synchronization system).

However, the demultiplexing process (recovering the original signals using the signals received by the DAQ) is a difficult task by factors such as crosstalk (interference between the multiplexed signals). Usually, filters are applied for signal demultiplexing. Nevertheless, filtering adds delays that affect the accurate estimation of the angular position and the stator currents. Demultiplexing techniques for motor drives are proposed in García et al. (2017, 2021). Synchronous current sampling can be used to recover the current signals: the data acquisition system, the resolver excitation signal, and the triangular carrier used in PWM are synchronized so that the resolver outputs are zero at the PWM carrier valleys (García et al., 2021). In that approach, the frequency of the resolver excitation voltage is half the switching frequency of the inverter used to control the three-phase motor. The distance between the spectra of the resolver outputs and the fundamental component of the current signals depends on the frequency of the resolver excitation voltage. In FDM, the greater that distance, the less the crosstalk effect. However, the resolver excitation frequency is less than the inverter switching frequency in the aforementioned approaches. As a result, the effect of crosstalk in angle estimation is increased when low inverter switching frequencies are applied.

This paper proposes an improved multiplexing approach to reduce the effect of crosstalk in angle estimation. At the same time, the synchronous current sampling can still be applied to get the stator current signals. In the proposed approach, the resolver excitation frequency is 1.5 times the inverter switching frequency, so the resolver outputs are zero when the PWM carrier reaches its valley. It is proved that the interference spectrum in the angle estimation produced by the current signal is centered at the resolver excitation frequency. Hence, interference is easier to reject if the excitation frequency becomes larger. Simulation tests were performed to compare the proposed multiplexing method with the approach applied in (García et al., 2018). Those tests prove that the proposed approach reduces the crosstalk effect in the angle estimation and allows recovering the current signals.

2. THEORETICAL FOUNDATIONS

2.1 Resolver Angular Position Sensor

Figure 1 describes the schematics of a wound-rotor resolver sensor. This sensor has a rotor winding and two perpendicular output stator windings. The rotor winding is mechanically coupled to the rotor shaft and receives a high-frequency sinusoidal voltage $v_e(t)$. Thus, the angle of this winding is equal to the motor shaft angle. This excitation voltage and the mechanical angle induce the voltages $v_s(t)$ and $v_c(t)$ in the output windings:

$$v_e(t) = a_e \cos(\omega_e t), \quad \omega_e = 2\pi f_e, \tag{1}$$
$$v_s(t) = k_r \sin(\theta(t)) v_e(t), \tag{2}$$
$$v_c(t) = k_r \cos(\theta(t)) v_e(t), \tag{3}$$

where

- a_e : resolver excitation amplitude (V).
- ω_e : resolver excitation frequency (rad/s).
- f_e : resolver excitation frequency (1 kHz to 15 kHz).
- t : time (s).
- k_r : rotor-stator transformation ratio (adimensional).
- $\theta(t)$: mechanical angle (rad/s).

The bandwidth of the resolver outputs (BW_r) are :

$$BW_r = 2max(\omega_m) \ (rad/s), \quad \omega_m << \omega_e, \tag{4}$$

where ω_m is the mechanical speed. Let $\mathcal{F}\{x(t)\}$ represents the Fourier transform of $x(t)$. Thus $\mathcal{F}\{\sin(\theta)\} = S(\omega)$ and $\mathcal{F}\{\cos(\theta)\} = C(\omega)$. The modulation property of Fourier transform allows expressing the spectra of $v_s(t)$ and $v_c(t)$ in terms of $S(\omega)$ and $C(\omega)$:

$$\mathcal{F}\{v_s(t)\} = 0.5 \left[S(\omega - \omega_e) + S(\omega + \omega_e) \right], \tag{5}$$
$$\mathcal{F}\{v_c(t)\} = 0.5 \left[C(\omega - \omega_e) + C(\omega + \omega_e) \right]. \tag{6}$$

Equations (4), (5) and (6) state that the resolver outputs are high-frequency signals whose spectra are narrow (respect to the mechanical speed) and centered at ω_e, as shown in Figure 2.

2.2 Stator Current Spectrum

Motor drives use three-phase inverters to give energy to three-phase motors. Let's consider that a modulation
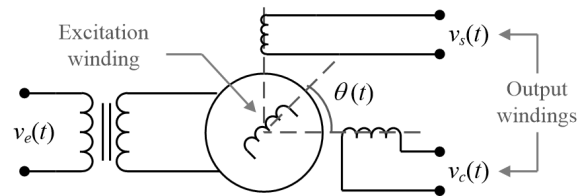
Figure 1. Wound-rotor resolver sensor.
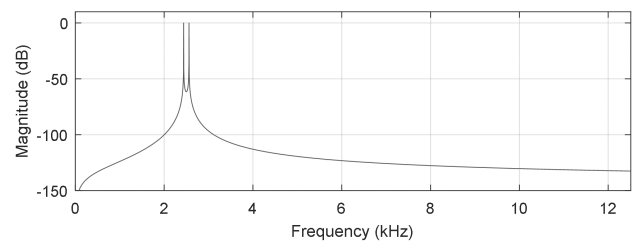
Figure 2. Spectrum of a resolver output ($f_e = 2.5$ kHz).

technique controls the inverter with a fixed switching frequency $\omega_{sw} = 2\pi f_{sw}$ (e.g., sinusoidal PWM or space vector PWM). In that case, the energy spectral density of the stator current is mainly concentrated at the fundamental frequency and near to integer multiples of the inverter switching frequency f_{sw}, as shown in Figure 3.

2.3 Frequency Division Multiplexing Applied in Motor Drives

Frequency division multiplexing (FDM) is a method in which band-limited signals with non-overlapping spectra are multiplexed through an additional process so that each signal occupies a different frequency band. (Haykin and Van Veen, 1998). Figures 2 and 3 show no overlap between the spectra of a stator current and a resolver output for practical applications. Thus, FDM can be applied to send those aforementioned signals to a single analog-to-digital converter (ADC).

Figure 4 describes the application of FDM in the DAQ of motor drives. Let $s_{i_a}(t)$, $s_{i_b}(t)$ be the output of the current sensors that measures the stator currents $i_a(t)$ and $i_b(t)$ after the signal conditioning process. Besides, let $s_{v_s}(t)$, $s_{v_c}(t)$ be the resolver outputs after the signal conditioning process. Equations (7) and (8) show how those signals are combined to produce the signals $s_{as}(t)$ and $s_{bc}(t)$ which are sent to the DAQ (García et al., 2021, 2017):

$$s_{as}(t) = s_{i_a}(t) + s_{v_s}(t), \qquad (7)$$
$$s_{bc}(t) = s_{i_b}(t) + s_{v_c}(t). \qquad (8)$$

Figure 5 shows the spectrum of $s_{as}(t)$. Note that the resolver output and the stator current are located in different frequency bands.

2.4 Demultiplexing of Stator Currents

Equations (7) and (8) show that multiplexing the resolver outputs and the current sensor signals is simple. However,
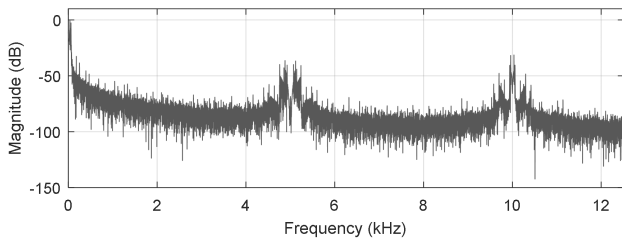
Figure 3. Spectrum of a stator current ($f_{sw} = 5$ kHz).
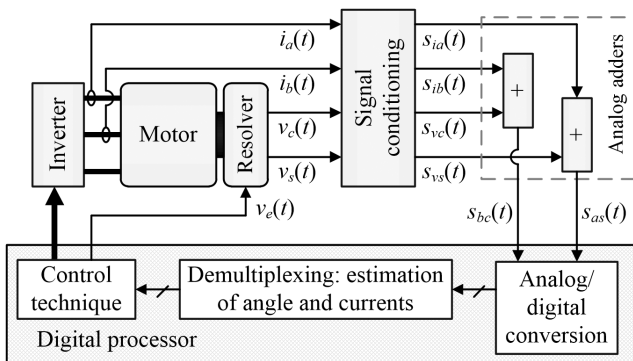
Figure 4. Application of FDM in motor drives.
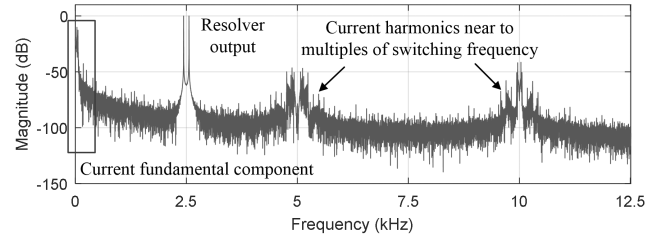
Figure 5. Sprectrum of $s_{as}(t)$.

the demultiplexing process is a difficult task. Commonly, pass-band filters are used to recover the signals multiplexed in the frequency domain. However, the filtering process adds delays into the resolver outputs and the current signals. Those delays may reduce the accuracy of the motor shaft angle estimation and the current control loop performance (García et al., 2017) .

Figure 6 illustrates the demultiplexing process explained in García et al. (2021), which is based on current synchronous sampling. Let t_i the instants when the triangular carrier used in PWM reaches its valleys. In the case of space vector PWM, t_i is located in the middle of the time interval when the zero voltage vector (V_0) is used (Briz et al., 2010). The data acquisition system, the resolver excitation signal, and the triangular carrier used in modulation are synchronized, such as the resolver output is zero at the PWM carrier valleys (i.e., when $t = t_i$). Therefore:

$$s_{v_s}(t_i) = 0 \rightarrow s_{as}(t_i) = s_{i_a}(t_i), \qquad (9)$$
$$s_{v_c}(t_i) = 0 \rightarrow s_{bc}(t_i) = s_{i_b}(t_i). \qquad (10)$$

Besides, according to synchronous current sampling theory, the current samples taken at the PWM peaks or valleys represent the fundamental components of the stator currents (Briz et al., 2010). As a result, $s_{as}(t_i)$ and $s_{bc}(t_i)$ are samples of the fundamental components of the stator currents. Many three-phase control techniques use only those fundamental components as the presence of the current harmonics may reduce the current control performance. Thus, the currents signals used in motor control, $i_{ad}(t)$ and $i_{bd}(t)$, are defined as follows:

$$i_{ad}(t) = s_{as}(t_i), \quad t_i \le t < t_{i+1}, \qquad (11)$$
$$i_{bd}(t) = s_{bs}(t_i), \quad t_i \le t < t_{i+1}. \qquad (12)$$
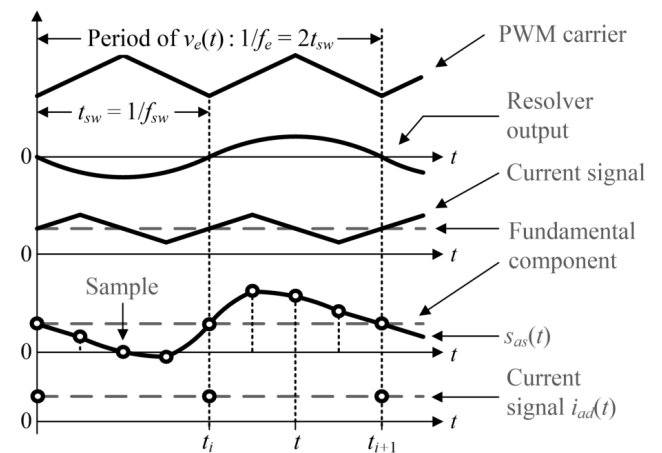
Figure 6. Demultiplexing of the current signals.

The aforementioned synchronization requires that the inverter switching frequency is twice the resolver excitation frequency:

$$f_{sw} = 2f_e. \tag{13}$$

2.5 Estimation of the Angular Position

The resolver signals can be demultiplexed using the signals $s_{as}(t)$, $s_{bc}(t)$ $s_{as}(t_i)$ and $s_{bc}(t_i)$ (García et al., 2021):

$$
\begin{aligned}
v_{se}(t) &= s_{as}(t) - s_{as}(t_i) \tag{14} \\
&= s_{v_s}(t) + \underbrace{s_{i_a}(t) - s_{i_a}(t_i)}_{r_1(t)},
\end{aligned}
$$

$$
\begin{aligned}
v_{ce}(t) &= s_{bc}(t) - s_{bc}(t_i) \tag{15} \\
&= s_{v_c}(t) + \underbrace{s_{i_b}(t) - s_{i_b}(t_i)}_{r_2(t)},
\end{aligned}
$$

where $v_{se}(t)$ and $v_{ce}(t)$ are the estimations of the resolver outputs. Considering that the digital processor used in vector control generates the resolver excitation voltage, then $v_e(t)$ is known. Let define $\theta_e(t)$ as the estimated angle. For simplicity, let assume that $a_e = 1$, $k_r = 1$, $s_{v_s}(t) = \sin(\theta(t))v_e(t)$, $s_{v_c}(t) = \cos(\theta(t))v_e(t)$, $v_e(t) = \cos(\omega_e t)$, $\theta(t) = \theta$, and $\theta_e(t) = \theta_e$. Thus, the term $\gamma(t)$ is calculated as follows (García et al., 2021):

$$
\begin{aligned}
\gamma(t) &= [v_{se}(t)\cos(\theta_e) - v_{ce}(t)\sin(\theta_e)]\, v_e(t) \tag{16} \\
&= [\sin(\theta)v_e(t)\cos(\theta_e) + r_1(t)\cos(\theta_e)]\, v_e(t) \\
&\quad - [\cos(\theta)v_e(t)\sin(\theta_e) + r_2(t)\sin(\theta_e)]\, v_e(t) \\
&= [\sin(\theta)\cos(\theta_e) - \cos(\theta)\sin(\theta_e)]\, v_e^2(t) \\
&\quad - \underbrace{[r_1(t)\cos(\theta_e) - r_2(t)\sin(\theta_e)]}_{p(t)}\, v_e(t) \\
&= \sin(\theta - \theta_e)v_e^2(t) + p(t)v_e(t).
\end{aligned}
$$

The angle estimation error is $e(t) = \theta(t) - \theta_e(t)$. If $e(t)$ is small, then $\sin(\theta(t) - \theta_e(t)) = \sin(e(t)) \approx e(t)$. Besides, $v_e^2(t) = \cos^2(\omega_e t) = 0.5 + 0.5\cos(2\omega_e t)$. Thus (16) can be rewritten as follows:

$$\gamma(t) \approx 0.5e(t) + 0.5e(t)\cos(2\omega_e t) + p(t)\cos(\omega_e t). \tag{17}$$

The modulation property of Fourier transform allows proving that $e(t)$ is a low-frequency signal, while the terms $e(t)\cos(2\omega_e t)$ and $p(t)\cos(\omega_e t)$ are high-frequency signals whose spectra are centered at $2\omega_e$ and ω_e, respectively, as shown in Figure 7. The angle tracking observer (ATO) used to estimate the angular position can be designed to act as a low-pass filter. Thus, the effect of $e(t)\cos(2\omega_e t)$ and $p(t)\cos(\omega_e t)$ will be rejected, and the angle estimation will mainly depend on $e(t)$. In (García et al., 2017) a type-III ATO is applied to get the angular positions from $\gamma(t)$, while a type-II ATO is applied in García et al. (2021).
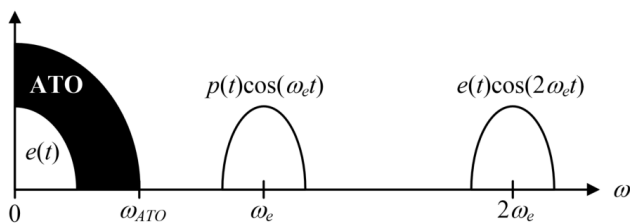
Figure 7. Spectra of $e(t)$, $e(t)\cos(2\omega_e t)$ and $p(t)\cos(\omega_e t)$.

3. PROPOSED IMPROVEMENT IN THE ANGLE ESTIMATION

The term $p(t)$ in (17) is produced by the current signals. Hence, $p(t)\cos(\omega_e t)$ is the interference of the current signals in the angle estimation. As mentioned before, the spectrum $p(t)\cos(\omega_e t)$ is centered at ω_e. If the value of ω_e increases, then the distance between the spectra of the signals $e(t)$ and $p(t)\cos(\omega_e t)$ becomes greater, making easier for the ATO to reject the current signal interference. On the other hand, the resolver outputs must be zero when the PWM triangular carrier reaches its valley, to recover each current fundamental component through synchronous sampling.

Figure 8 explains the proposed multiplexing approach to increase the resolver excitation frequency, while it is possible to apply synchronous current sampling. Note that

$$3/f_e = 2/f_{sw} \tag{18}$$

Hence, the resolver excitation frequency is 1.5 times the inverter switching frequency, as indicated in (19). Under this condition, the PWM carrier and the resolver excitation can still be synchronized so that the resolver outputs become zero at the PWM carrier valleys. Thus, (11) and (12) can be applied to get the fundamental component of each stator current.

$$\omega_e = 1.5\omega_{sw}, \quad f_e = 1.5f_{sw} \tag{19}$$

4. RESULTS

The proposed approach was tested using simulations performed in MATLAB. The parameters of the resolver and the type-II ATO used in the simulation are the same as described in (García et al., 2018):

- $a_e = 1$.
- $f_{sw} = 5$ kHz.
- $k_r = 1$.
- ATO gains: 640, 7.87×10^5, 5.99×10^7.
- Resolver excitation frequency for the proposed approach based on (19): f_e=7.5 kHz.
- Resolver excitation frequency in García et al. (2018): $f_e = 2.5$ kHz.
- The stator currents and resolver sensors were normalized in the range $[-1, +1]$ p.u.
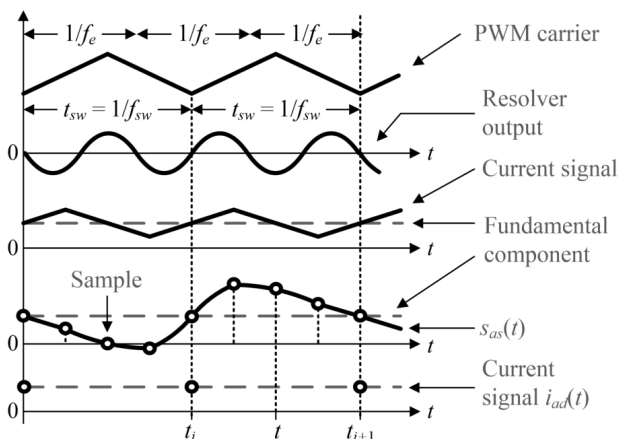
Figure 8. Proposed multiplexing approach.

Figure 9 shows the mechanical speed used in simulations. Figures 10 and 11 show the actual and the estimated stator currents $i_a(t)$ and $i_b(t)$. Figure 12 is the amplification of Figure 11. Note that the current signal obtained through synchronous current sampling accurately estimates the stator current fundamental component (the harmonics have been attenuated).

Figures 13 and 14 compare the proposed multiplexing approach using $f_e = 7.5$ kHz with the approach in (García et al., 2018) where $f_e = 2.5$. The same ATO was used for both tests. Besides, the estimated angle from each
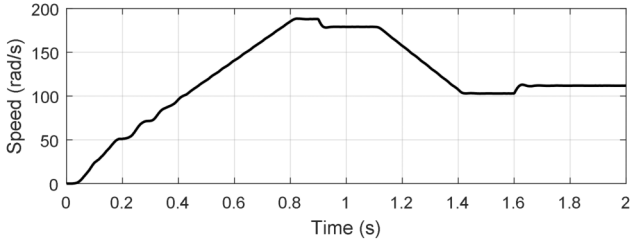
Figure 9. Mechanical speed used in simulations.
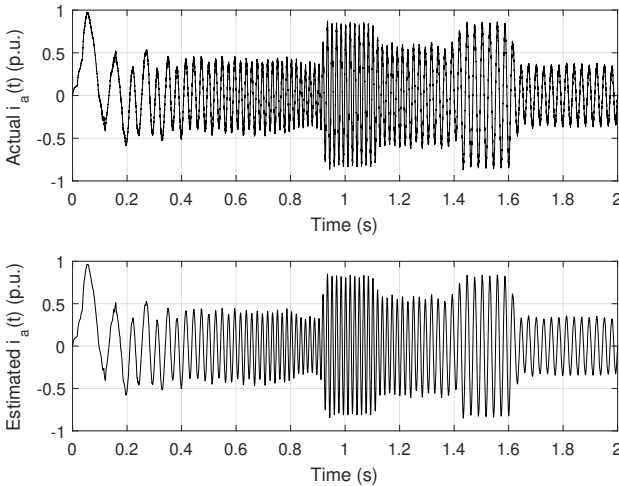
Figure 10. Estimation of the fundamental component of $i_a(t)$.
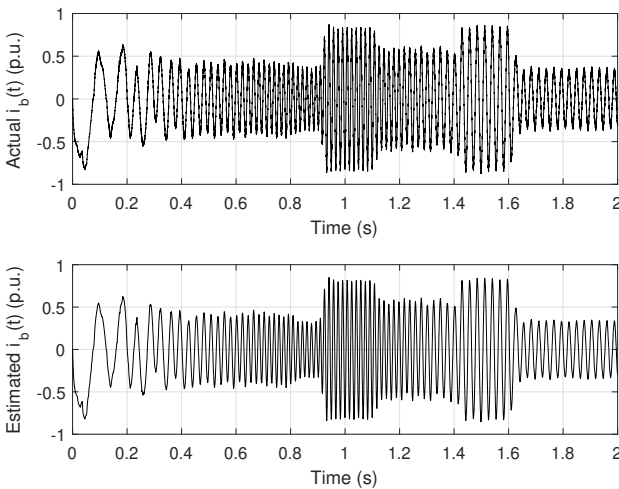
Figure 11. Estimation of the fundamental component of $i_b(t)$.
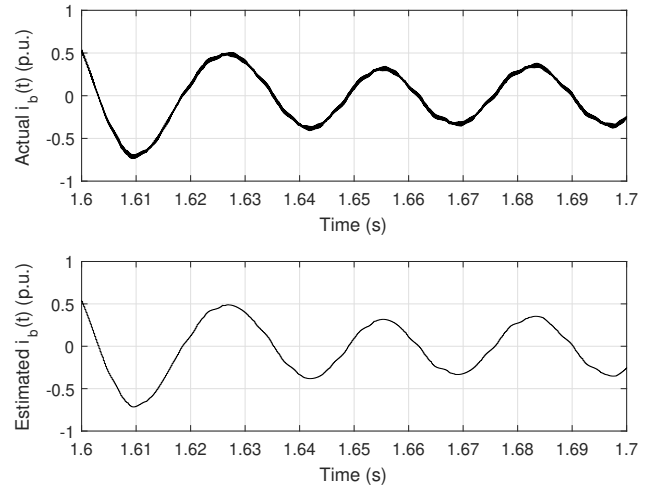
Figure 12. Estimation of the fundamental component of $i_b(t)$ (amplification).
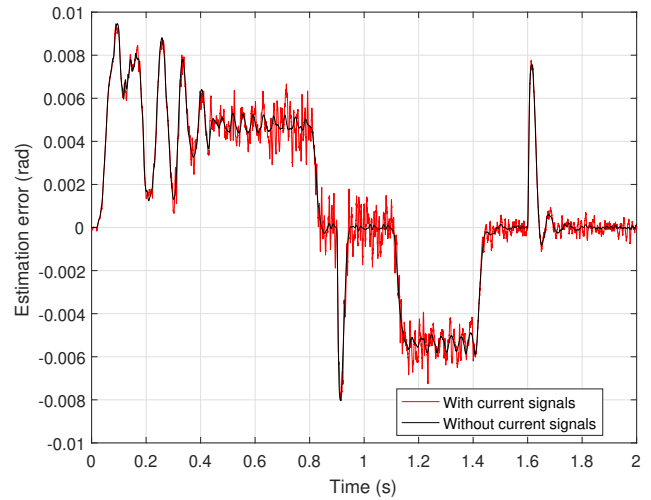
Figure 13. Angle estimation error using $f_e = 2.5$ kHz, as in (García et al., 2018) .
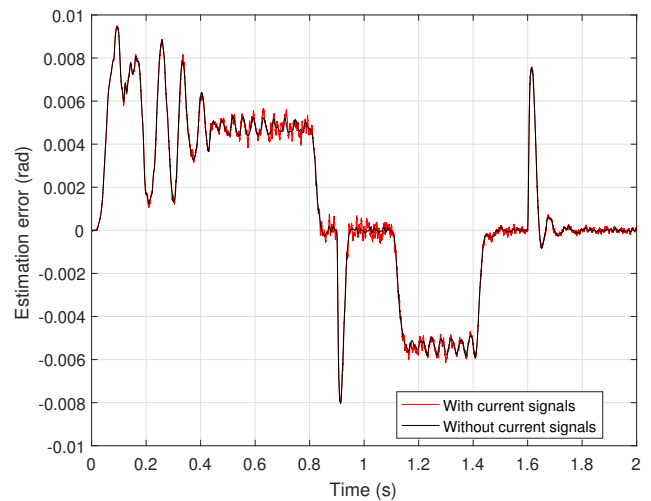
Figure 14. Angle estimation error using $f_e = 7.5$ kHz, using the proposed approach.

approach is compared with the angle estimation error when FDM is not applied to verify the effect of crosstalk in each test. Note that the angle estimation ripple was

reduced for the proposed approach. The root mean square error (RMSE) for each test from $t = 1.8s$ to $t = 2s$ (error in steady-state conditions) was calculated:

- RMSE for the proposed approach: 8.06×10^{-5}.
- RMSE for García et al. (2018): 2.48×10^{-4}.

Those results indicate that the proposed approach reduces the crosstalk effect in angle estimation.

5. CONCLUSIONS

This paper presents a novel multiplexing strategy to get the angular position from the resolver and the current signals when frequency division multiplexing (FDM) is applied in the motor drive data acquisition system. Increasing the resolver excitation frequency increases the distance between the spectra of the resolver output and the stator currents. Thus, the effect of crosstalk in angle estimation is reduced. The proposed approach is practical when low inverter switching frequencies are used. Commercial resolvers have excitation frequencies up to 15 kHz. Hence, it is possible to get an adequate resolver to implement the proposed approach. In future work, the proposed multiplexing approach will be tested experimentally.

ACKNOWLEDGE

REFERENCES

Ali, N., Gao, Q., and Ma, K. (2020). A cost-effective dual bus current measurement scheme for current control of three-phase switched reluctance motors. In *2020 IEEE 9th International Power Electronics and Motion Control Conference (IPEMC2020-ECCE Asia)*, 2562–2566. doi:10.1109/IPEMC-ECCEAsia48364.2020.9367882.

Briz, F., Díaz-Reigosa, D., Degner, M.W., García, P., and Guerrero, J.M. (2010). Current sampling and measurement in pwm operated ac drives and power converters. In *The 2010 International Power Electronics Conference - ECCE ASIA -*, 2753–2760. doi:10.1109/IPEC.2010.5543175.

García, R.C., Pinto, J.O.P., Suemitsu, W.I., and Soares, J.O. (2017). Improved demultiplexing algorithm for hardware simplification of sensored vector control through frequency-domain multiplexing. *IEEE Transactions on Industrial Electronics*, 64(8), 6538–6548. doi:10.1109/TIE.2017.2682780.

García, R.C., Filho, F.J.T., Pinto, J.O.P., Suemitsu, W.I., Fonseca, B.S.d., and Brun, A.D.M. (2021). Improved acquisition system for sensored vector control through frequency-domain multiplexing, synchronous sampling, and differential evolution. *IEEE Sensors Journal*, 21(6), 7784–7792. doi:10.1109/JSEN.2020.3045372.

García, R.C., Pinto, J.O.P., Ono, I.E.S., Fahed, V.d.S., and Brito, M. (2018). Simplification of the acquisition system for sensored vector control using resolver sensor based on fdm and current synchronous sampling. In *2018 IEEE 4th Southern Power Electronics Conference (SPEC)*, 1–7. doi:10.1109/SPEC.2018.8635967.

Haykin, S. and Van Veen, B. (1998). *Signals and Systems*. Wiley.

Jang, P., Lee, T., Hwang, Y., and Nam, K. (2022). Quadrature demodulation method for resolver signal processing under different sampling rate. *IEEE Access*, 10, 7016–7024. doi:10.1109/ACCESS.2021.3136770.

Lara, J., Xu, J., and Chandra, A. (2016). Effects of rotor position error in the performance of field-oriented-controlled pmsm drives for electric vehicle traction applications. *IEEE Transactions on Industrial Electronics*, 63(8), 4738–4751. doi:10.1109/TIE.2016.2549983.

Lee, S., Kim, H., and Lee, K. (2022). Current measurement offset error compensation in vector-controlled spmsm drive systems. *IEEE Journal of Emerging and Selected Topics in Power Electronics*, 10(2), 2619–2628. doi:10.1109/JESTPE.2022.3151351.

Modesto, P., Estrabis, T., and Cordero, R. (2020). Analysis about the application of frequency-domain multiplexing in data acquisition for vector control. In *2020 IEEE XXVII International Conference on Electronics, Electrical Engineering and Computing (INTERCON)*, 1–4. doi:10.1109/INTERCON50315.2020.9220216.

Naderi, P., Ramezannezhad, A., and Vandevelde, L. (2022). A novel linear resolver proposal and its performance analysis under healthy and asymmetry air-gap fault. *IEEE Transactions on Instrumentation and Measurement*, 71, 1–9. doi:10.1109/TIM.2022.3155747.

Raja, R., Sebastian, T., Wang, M., Gebregergis, A., and Islam, M.S. (2017). Effect of position sensor error on the performance of permanent magnet machine drives. *IEEE Transactions on Industry Applications*, 53(6), 5518–5526. doi:10.1109/TIA.2017.2704898.

Saneie, H., Nasiri-Gheidari, Z., and Tootoonchian, F. (2020). Structural design and analysis of a high reliability multi-turn wound-rotor resolver for electric vehicle. *IEEE Transactions on Vehicular Technology*, 69(5), 4992–4999. doi:10.1109/TVT.2020.2981551.

Wang, S., Kang, J., Degano, M., and Buticchi, G. (2019). A resolver-to-digital conversion method based on third-order rational fraction polynomial approximation for pmsm control. *IEEE Transactions on Industrial Electronics*, 66(8), 6383–6392. doi:10.1109/TIE.2018.2884209.